Climatic-induced spatio-temporal change of kinematics and ground temperature of rock glaciers and permafrost in the Hohe Tauern Range, Austria

Andreas Kellerer-Pirklbauer[1,2], Michael Avian[1], Viktor Kaufmann[1], Erich Niesner[3†] & Birgit Kühnast[4]

(1) Institute of Remote Sensing and Photogrammetry, Graz University of Technology, Austria
(2) Department of Geography and Regional Science, University of Graz
(3) Department of Applied Geological Sciences and Geophysics, University of Leoben, Austria
(4) KNGeolektrik e.U., Leoben, Austria

1 Introduction

High altitude and high latitude regions are generally recognized as being particularly sensitive to the effects of the ongoing climate change (e.g. French 1996, Haeberli et al 1993). A large part of permafrost, permafrost-related active rock glaciers and glaciers in the European Alps are for instance at or close to melting conditions and therefore very sensitive to degradation or to disappearance caused by atmospheric warming. Knowledge regarding permafrost distribution and its climatologically driven dynamics in the entire European Alps is still far from being complete although promising modelling approaches for this scale exist (Boeckli et al. 2012).

Active rock glaciers are creep phenomena of continuous and discontinuous permafrost in high-relief environments moving slowly downvalley or downslope (Barsch 1996, Haeberli et al. 2006, Berthling 2011). Rock glaciers are often characterised by distinct flow structures with ridges and furrows at the surface with some similarity to the surface of pahoehoe lava flows. At steeper parts or at the front of a rock glacier, the rock glacier body might start to disintegrate (e.g. Avian et al. 2009) or even completely tear apart and collapse (Krysiecki et al. 2008). Over time and during climate warming, an active rock glacier might turn first to inactive (widespread permafrost, no movement), second to pseudo-relict (sporadic to isolated permafrost, no movement) and finally to relict (no permafrost, no movement) (Barsch 1996, Kellerer-Pirklbauer 2008).

The projects ALPCHANGE (2006–2011; funded by the Austrian Science Fund FWF) and PermaNET (2008–2011; co-funded by the European Union within the Alpine Space framework) formed major basis in terms of data and expertise for the permAfrost project. Within ALPCHANGE a comprehensive monitoring network was established in the Hohe Tauern Range, Austria. These devices operate successfully since summer 2006 and delivered promising results since then. Furthermore and with regards to content, important long-term monitoring activities such as (i) geodetic surveys of particular rock glaciers (started in 1995), (ii) terrestrial laser scanning (TLS) of a rock glacier (started in 2000) and rock walls in permafrost conditions (started in 2009) as well as (iii) monitoring of the thermal regime of the ground (started 2006) were continued within the permAfrost project.

Research within permAfrost aimed to continue and improve previously carried out research in the field of kinematics, volumetric and thermal monitoring of rock glacier and permafrost and to understand the inner structure of rock glaciers applying a combination of geophysical methods. Thereby, research focused particularly on the rock glaciers Weissenkar (WEI), Hinteres Langtalkar (HLC) and Dösen (DOE) all located in the Hohe Tauern Range, Austria. These rock glaciers are of special interest for rock glacier research because they are one of the best studied rock glaciers in Austria but also to some extent of the European Alps. Furthermore, data and expertise gathered during the project period 2010 to 2013 from other study areas in the Hohe Tauern Range were also used in this study for result optimization. Therefore the aim of this project was to provide a deeper insight into kinematics, morphodynamics and thermal state of the three rock glaciers and their close vicinity by using a multidisciplinary approach

applying geodesy, aerial photogrammetry, TLS, geophysical techniques and automatic monitoring.

2 Study areas

The three studied rock glaciers WEI, HLC and DOE are all located in the Tauern Range in Austria. The Tauern Range is an extensive mountain range in the central part of the Eastern Alps covering 9 500 km² in Austria and Italy and is commonly separated into the Hohe Tauern Range and the smaller Niedere Tauern Range. The former covers ca. 6 000 km² and reaches with Mt. Großglockner 3 798 m a.s.l. the highest summit of Austria. As mentioned above, this research project focuses on three different rock glaciers in the Hohe Tauern Range, two of them are located in the sub-unit Schober Mountains and one in the sub-unit Ankogel Mountains. Figure 1 gives an overview about the studied rock glaciers. Figure 2 shows detailed maps of the three rock glaciers with spatial information about instrumentation and measurements.

The three rock glaciers can be briefly characterised as further below. For detailed description and overview about previous research at these rock glaciers see Kellerer-Pirklbauer and Kaufmann (2012).

Weissenkar Rock Glacier (WEI): N 46° 57', E 12° 45'; elevation range from 2 620 to 2 870 m a.s.l. with a length of 650 m and a width of 300 m. WEI is a slowly moving tongue-shaped rock glacier consisting of an upper lobe overriding a lower lobe and characterized by well developed furrows and ridges at the entire lower half of the rock glacier. WEI moves up to 11 cm / a at present.

Hinteres Langtalkar Rock Glacier (HLC): N 46° 59', E 12° 47'; elevation range from 2 455 m to 2 720 m a. s. l. with a length of 900 m and a width of 300 m. HLC is a very active, monomorphic tongue-shaped rock glacier with two rooting zones. Distinct changes of the rock glacier surface were detected on aerial photographs from 1997 on (Avian et al. 2005). The movement pattern since 1997 differentiates a slower upper part and a substantially faster lower part with maximum horizontal displacement rates up to 250 cm/a. Therefore, HLC is one of the currently fastest moving rock glaciers in Europe (Delaloye et al. 2008) and possibly in the world underlining the high importance of research continuation.

Dösen Rock Glacier (DOE): N 46° 59', E 13° 17'; elevation range from 2 355 to 2 650 m a. s. l. with a length of 950 m and a width of 250 m. DOE is an active, monomorphic tongue-shaped rock glacier situated at the end of the glacially shaped, W-E oriented inner Dösen Valley. Displacement measurements (horizontal and vertical) started at this site in 1995 revealing mean surface velocity rates of up 13 to 37 cm/a.

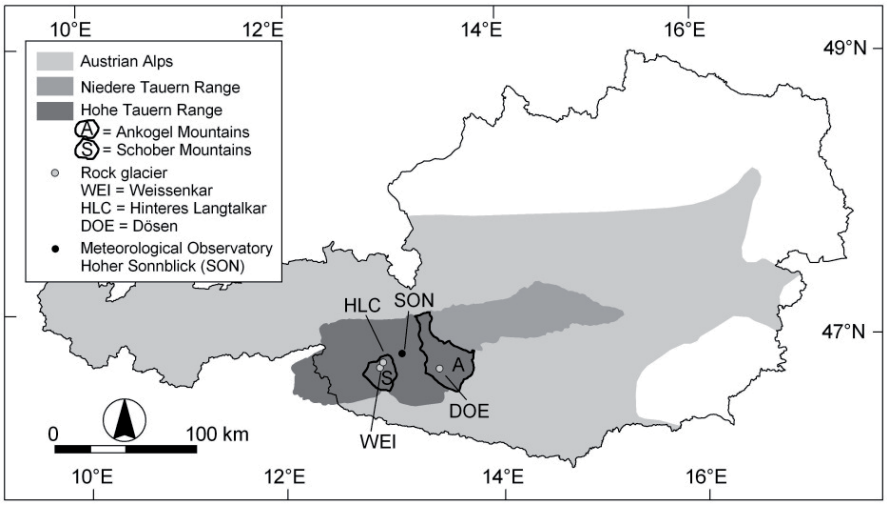

Figure 1: Location of the three rock glaciers Weissenkar (WEI), Hinteres Langtalkar (HLC) and Dösen (DOE) in the Hohe Tauern Range, central Austria. WEI and HLC are located in the sub-unit Schober Mountains, DOE in the Ankogel Mountains. Location of the Meteorological Observatory Hoher Sonnblick (SON) is indicated. The proximity of the three rock glaciers to SON was a big advantage for our analyses because of long-term climatic data series

3 Methods

3.1 3D-kinematics of rock glacier

3.1.1 Maintenance of geodetic networks

The geodetic networks of the three rock glaciers consist of stabilized points, mounted either on stable or non-stable, i. e. moving, ground (Fig. 2). For better identification of these points in the field red paint is used to mark and to enumerate them clearly. The maintenance work carried out on an annual basis consisted of (1) check of point existence, (2) check of point stability, (3) exchange of rusty screws, (4) lubrication of the screws, (5) renewal of faded red paint, and (6) renewal / placement of cairns for faster point identification.

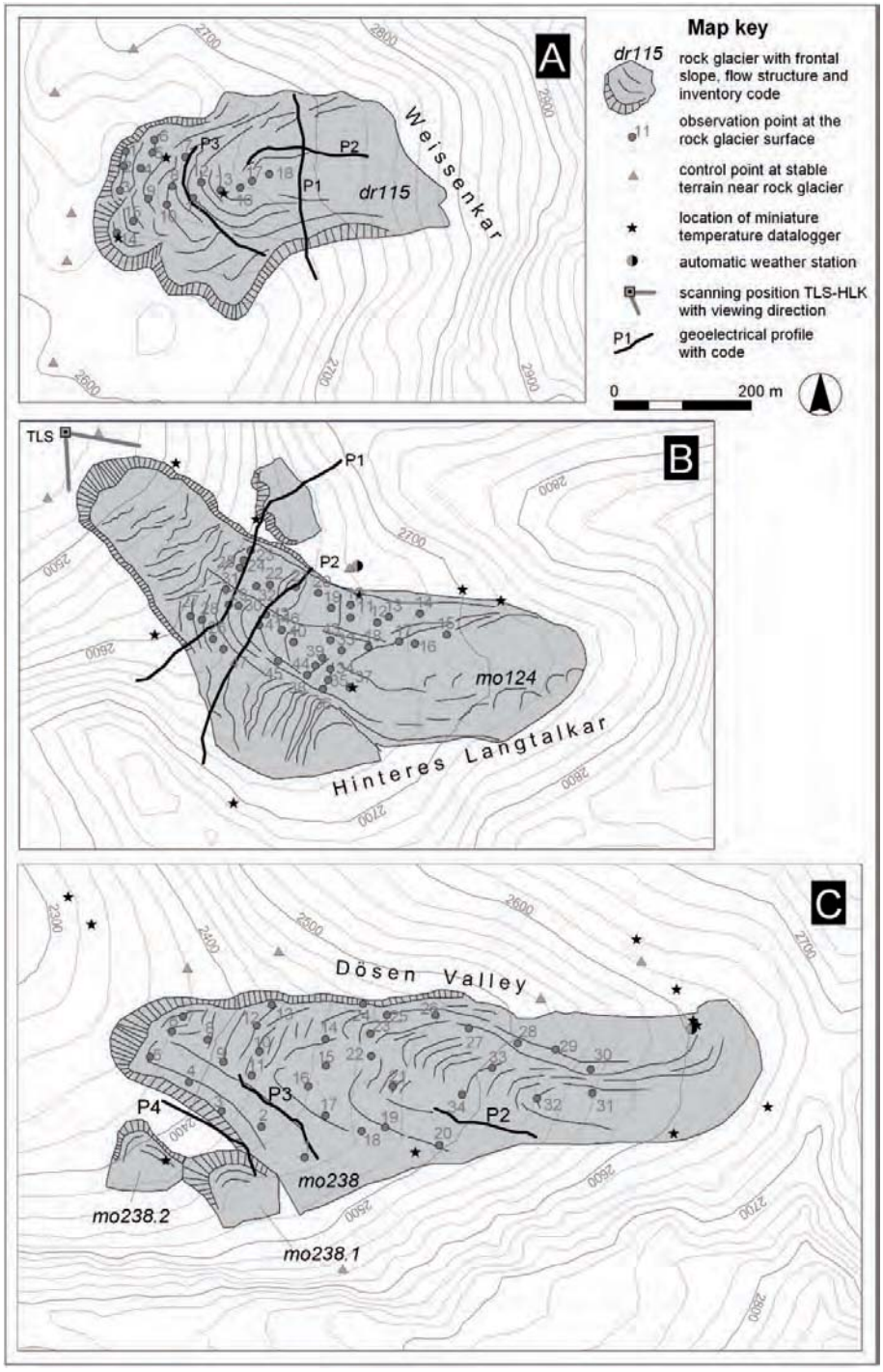

Figure 2: Morphology of the three rock glaciers WEI (A), HLC (B) and DOE (C) with locations of relevant instrumentations and measurement sites. These are locations for geodetic monitoring (observation points at the rock glacier surface and stable control points), locations of miniature temperature data logger (MTD; partly shown – some are outside the depicted maps) and automatic weather stations (AWS), position of the terrestrial laser scanner (TLS) at HLC and locations of the geoelectrical profiles. Locations of very low frequency (VLF) electromagnetic measurements are not indicated. Rock glacier codes according to the inventory by Lieb et al. (2010) described in Kellerer-Pirklbauer et al. (2012)

3.1.2 Annual geodetic measurements

For the geodetic monitoring (deformation analysis of the rock glacier bodies) appropriate geodetic networks consisting of stable reference points in the surroundings of the rock glacier and observation points on the rock glacier were available. The geodetic measurements from 2010 to 2012 were carried out following the proven scheme of the previous years (Kienast and Kaufmann 2004). The geodetic equipment consisted of a Total Station 1201 of Leica (Fig. 3). Leica circular prisms (geodetic reflectors) were used for point signalling. Data evaluation was done in the office using standard geodetic software (Geosi 6.0). Co-ordinate lists of all observation points of the three rock glaciers were prepared for each of the three epochs. Point accuracies obtained are in the order of ± 1 cm. As a result, annual 3 D displacement vectors were computed for all observation points. Products derived therefrom are 2 D displacement vectors, annual horizontal flow velocities, strain rates, and other key figures of surface deformation.

3.1.3 Photogrammetric surface deformation measurement

Aerial photogrammetry enables area-wide mapping of surface change. Multi-temporal aerial photographs can be used to detect and measure surface movement. Surface change can be described using 2 D or 3 D displacement vectors. Knowing the time span between two overflights, change rates, i. e. velocities, can be derived thereof. The successful implementation of a stringent algorithm for computing 3 D displacement vectors using multi-temporal digital aerial photographs was demonstrated by Kaufmann and Ladstädter (2003).

In the framework of the present project, however, the authors applied a modified algorithm which computes 2 D displacement vectors based only on high-resolution inter-annual orthophotos taken from virtual globes. Such orthophotos are generally free of charge. However, appropriate orthoimages (high resolution, good radiometry, multi-temporal, known acquisition dates) are scarce. The applicability of the proposed method has been shown for several rock glaciers in the Schober Mountains, Hohe Tauern (Kaufmann 2010, Kaufmann et al. 2012). For reasons of comparison this method was also evaluated at HLC and at Äußeres Hochebenkar rock glacier, Ötztal Alps (Kaufmann 2012). The results obtained for HLC are presented in this report.

Figure 3: Total Station TCRA 1201 of Leica operated in the field

3.1.4 Terrestrial laser scanning (TLS)

Usage of TLS on rock glaciers in the European Alps started at the beginning of this millennium (Bauer et al. 2003) and allows acquiring 3 D surface data with high spatial sampling rate. TLS is a time-of-flight system that measures the elapsed time of the laser pulse emitted by a photodiode until it returns to the receiver optics. Maximum range mainly depends on the reflectivity of surface (which is excellent for snow, rock or debris), and atmospheric visibility (best for clear visibility, bad for haze and fog). Since each single measurement consists of a multitude of laser returns, different measurement modes (first return, last return, strongest return) give proper results even during bad weather conditions and on poor surfaces that may otherwise lead to ambiguous measurements like vegetated, moist or roughly structured terrain (Baltsavias et al. 1999).

Long-range TLS (more than 400 m) is of particular interest for measuring high mountain environments as it offers very detailed digital surface models in non-accessible terrain (Bauer et al. 2003). A (theoretical) measuring range of up to 2000 m (RIEGL LMS Z620) allows hazardous sites to be easily measured from a safe distance. Despite these advantages, TLS has rarely been used in characterizing rock glacier movement (Bodin et al. 2008, Avian et al. 2009)

In 2003 the University of Graz joined JOANNEUM Research Graz in a set of experiments using this new technology for monitoring glaciers and rock glaciers in the Austrian Alps. However, first measurements at the rock glacier HLC and at the Gößnitz Glacier were carried out in summer 2000. First measurements at Pasterze Glacier followed in 2001. All these measurements were carried out using the instrument Riegl LPM–2k (e.g. Bauer et al. 2003, Kellerer-Pirklbauer et al. 2005, Avian et al. 2008, 2009). The recent measurements at HLC (Fig. 4) were carried out within the framework of permAfrost.

From 2009 on a new system (instrument Riegl LMS-Z620) has been used to reduce acquisition time as well aground sampling distance and hence increase point density. Digital Terrain Models (DTM) derived from data of different measurements can be subsequently compared to get a full description of changes in volume, surface dynamics, spatial distribution of shape, or arbitrary profiles on the surface. The filtering and registration of the measured point clouds was conducted in RIEGL RiScan. To avoid misinterpretations all point clouds were matched with the software LS3D (Akca 2010). As reference data set the point cloud measured in 2009 was considered.

3.2 Internal structure of rock glaciers: Geophysics

3.2.1 Very low frequency electromagnetic measurements (VLF)

The VLF method measures the components of the magnetic field of an electromagnetic wave. This electromagnetic wave is transmitted in the majority by military transmitters. The primary purpose of these transmitters with spatial ranges of 4 000 to 5 000 km is to communicate with submarines. The transmitters are installed worldwide. The low frequencies between 15 to 20 kHz had been chosen to get a larger skin depth of the waves. Therefore the depth of penetration of these waves is, compared to waves with higher frequency, deeper.

For geophysical purposes the base wave can be used very well for prospection. The magnetic component of the wave penetrates also deeper into the subsurface. When there are conductive bodies a local change in the amplitude and phase of this magnetic vector is resulting due to the development of secondary fields. In this measurement method the changes of the magnetic component – in this case the tilt angle and the phase shift – are measured by a receiver. Analysing these data by Fraser or Karous-Hjelt filter-

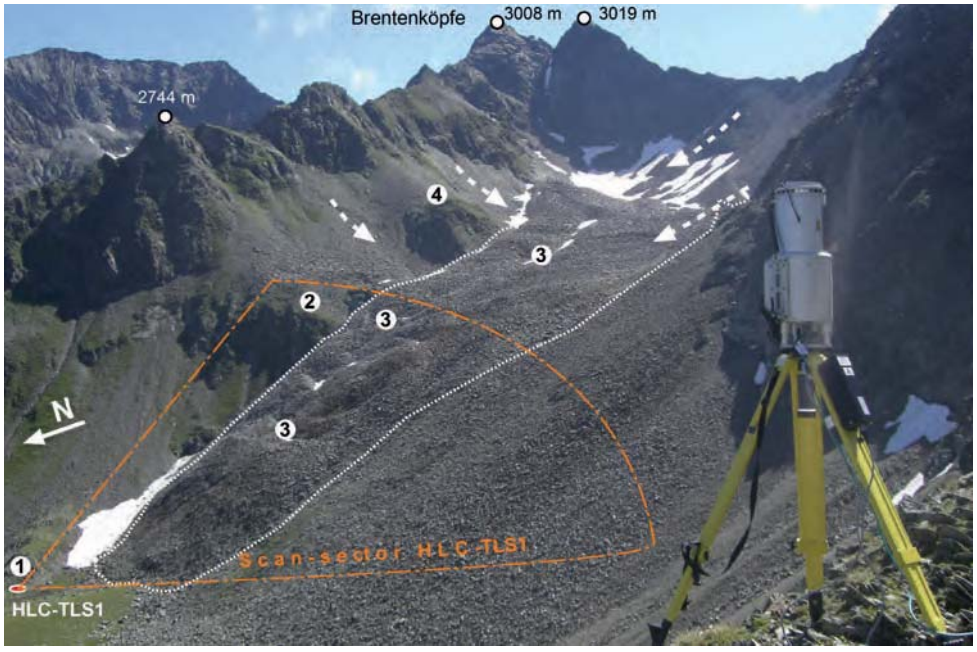

Figure 4: Terrestrial Laser Scanner RIEGL LMS Z620 in front of the rock glacier HLC at the scanning position HLC_Grat (which was not considered in this study). Codes: (1) Scanning position HLK-TLS1 at the rock glacier front, (2) prominent terrain ridge, (3) transversal furrows/crevasses, (4) location of the automatic weather station. White dotted arrows indicate potential rock glacier nourishment paths at HLC

ing (Karous and Hjelt 1977), conductive zones in the subsurface can be detected. We achieve the best resolution with this method when the magnetic vector is normal to the geologic striking. For the current prospection the best suited transmitter in direction and signal strengths is the VLF-transmitter JXZ (Helgeland, Norway) with a frequency of 17.1 kHz. For the field measurements a VLF-receiver type EM16 from the company Geonics had been used.

3.2.2 Direct current resistivity measurements (DC)

The geoelectric method measures the resistivity of the subsurface by sending electric current into the subsurface using two electrodes and measuring the resulting voltage at two other electrodes. Applying Ohm'schs law and including the geometry of the electrode layout the resistivity of the subsurface and the 3 D distribution can be calculated (Kneisel and Hauck 2008). The depth of penetration can be controlled by the distance between the electrodes – large electrode distances give information on deeper layers as the current can penetrate deeper into the subsurface. A shifting in the electrode layout results in lateral resistivity changes along the profile.

Depending on the task 1 D, 2 D or 3 D measurements can be applied. If also temporal changes using repeat measurements are included the measurements are called 4 D-measurements. In the current case 2 D-measurements had been applied (measurement system from LGM, Germany). The changes of the electrode positions are automatically controlled by computer. With this automatic measurement system a higher amount of data can be measured in shorter time compared to the manual method. The coverage of the subsurface is therefore increased. In measuring deeper zones by increasing the electrode distances also the shallower layers contribute to the measuring signal, therefore the measured data had to be inverted to separate the individual influences. For further information on the method such as limitations and equivalence we refer to e. g. Koefoed (1979) or Kneisel and Hauck (2008).

3.3 Permafrost and climate monitoring

3.3.1 Climate monitoring

The main devices used in the permafrost monitoring network at the three study areas are (1) automatic energy-balance monitoring stations or automatic weather stations (AWS), (2) miniature temperature data loggers (MTD) for monitoring ground surface and near ground surface temperature, and (3) automatic remote digital cameras (RDC).

The two AWS were installed in 2006 at the rock glaciers DOE and HLC within the ALPCHANGE project (Fig. 5). At both stations, climate data including air temperature, air humidity, wind speed (max, mean), wind direction and global radiation are continuously logged since then although major technical problems caused data gaps. No station exists at the rock glacier WEI, but due to its close distance to HLC (less than 4 km) and the same elevation range, the climate data collected at the rock

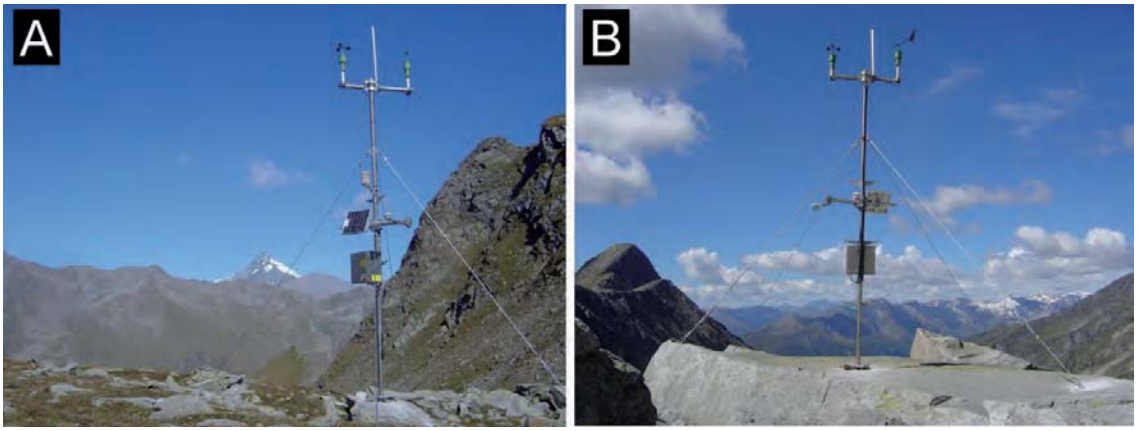

Figure 5: The AWS at the rock glaciers HLC (A) and DOE (B) installed in 2006. The station at HLC is located on bedrock at 2 655 m a. s. l. in close vicinity to the rock glacier. The station at DOE is located on a large boulder on the rock glacier surface at 2 600 m a. s. l. Photograph viewing directions towards NW (A) and W (B). Note Mt. Großglockner (3 798 m a.s.l.) in the background of (A)

Table 1: The 27 MTD-sites at the three study areas where ground surface and near surface temperature was monitored during the permAfrost WP4000 project period. Different parameters are indicated for each site. Furthermore, the available data series since 1 June 2010 are listed. Substrate abbreviations: FGM = fine-grained material, CGM = coarse-grained material, BED = bedrock. For locations see Figure 6

Area	MTD-site	Description	Substrate	Elevation [m a. s l.]	Aspect [°]	Slope [°]	Sensor depth(s) [cm]	Data series
HLC	HLC-LO-S	debris slope	CGM	2 489	245	32	0	010610-220812
	HLC-MI-S	debris slope	CGM	2 581	268	19	0	010610-220812
	HLC-UP-S	debris slope	CGM	2 696	256	22	0	010610-220812
	HLC-LO-N	rock wall niche with debris	BED	2 485	47	45	0	010610-220812
	HLC-MI-N	debris slope	CGM	2 601	17	28	0	010610-220812
	HLC-UP-N	rock wall niche with debris	BED	2 693	45	52	0	010610-220812
	HLC-RF-S	rock face	BED	2 725	241	75	3, 10, 40	010610-220812
	HLC-RF-N	rock face	BED	2 693	45	85	3, 10, 40	010610-220812
	HLC-RT	flat bedrock site	BED	2 650	252	7	3, 10, 40	010610-220812
	HLC-CO	rock glacier sediments	CGM	2 672	338	8	3, 10, 100	010610-220812
	HLC-SO-S	solifluction lobe	FGM	2 391	253	34	0, 10, 40	010610-220812
	HLC-SO-N	solifluction lobe	FGM	2 407	34	33	0, 10, 40	010610-220812
WEI	WEI-LO	rock glacier sediments	CGM	2 652	238	22	0	010610-210812
	WEI-MI	rock glacier sediments	CGM	2 662	270	3	0, 30, 100	010610-210812
	WEI-UP	rock glacier sediments	CGM	2 688	241	7	0	010610-210812
DOE	DOV-LO-S	debris slope	CGM	2 489	220	22	0	250806-200812
	DOV-MI-S	rock wall niche with debris	BED	2 586	213	19	0	010610-200812
	DOV-UP-S	debris slope	CGM	3 002	166	33	0	010610-300611 & 160811-200812
	DOV-LO-N	debris slope	CGM	2 407	342	22	0	010610-200812
	DOV-MI-N	debris slope	CGM	2 501	239	16	0	010610-200812
	DOV-UP-N	debris slope	CGM	2 626	331	25	0	010610-200812
	DOV-RF-S	rock face	BED	2 628	206	80	3, 10, 32	010610-200812
	DOV-RF-N	rock face	BED	2 638	300	90	3, 10, 40	010610-230711 & 160811-200812
	DOV-RT	flat bedrock site	BED	2 603	255	14	3, 10, 40	010610-200812
	DOV-CO*	rock glacier sediments	CGM	2 606	257	5	100, 200, 300	010610-200812
	DOV-FI	slope with vegetation	FGM	2 644	213	28	0, 3, 10, 30, 70, 100	010610-200812
	DOV-SO	solifluction lobe	FGM	2 578	116	18	3,10,70	No data

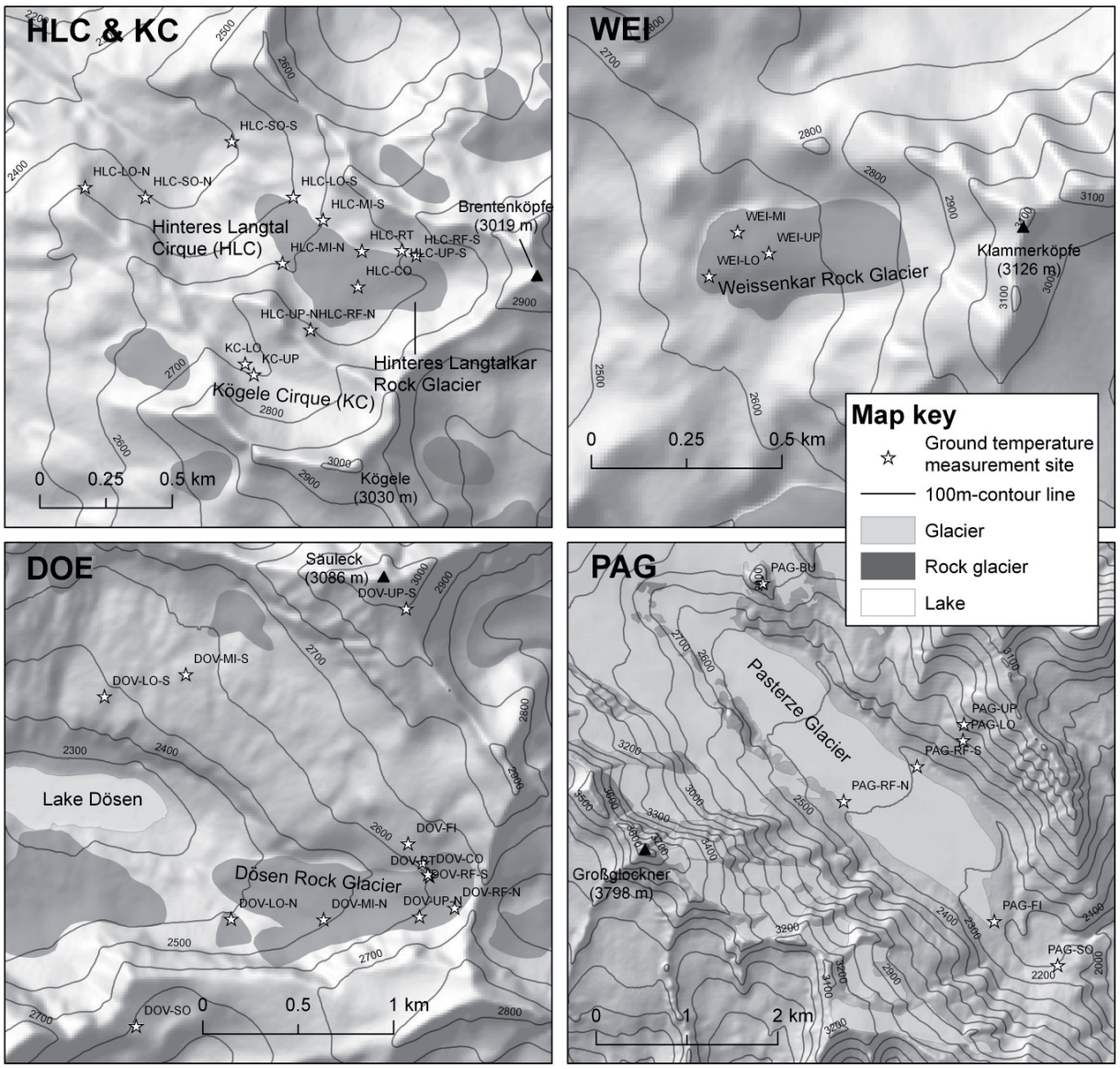

Figure 6: Detailed maps of the three main study areas HLC, WEI and DOE as well as of two additional study areas at KC (Kögele Cirque) and PAG (Pasterze Glacier) with the locations of ground temperature measurement sites using miniature temperature datalogger (MTD). For details and description of the MTD sites at the three main study areas refer to Table 1

glacier HLC are presumably also valid for the rock glacier WEI. However, solely air temperature at WEI was measured in the period from 2011 to 2012 for comparison.

3.3.2 Ground temperature monitoring

About 30 miniature temperature data loggers (MTD) for monitoring ground surface, near ground surface and air temperature were installed in 2006 and later at the three rock glacier sites. The used MTDs are either 1-channel data loggers (GeoPrecision, Model M-Log1) monitoring with one temperature sensor or 3-channel data loggers (GeoPrecision, Model M-Log6) monitoring with three sensors at different depths. According to the manufacturer, the used PT1000 temperature sensors have an accuracy of ± 0.05 °C, a range of – 40 to + 100 °C and a calibration drift of < 0.01 °C / a. Generally, the MTDs were funded by the ALPCHANGE project.

Within the following PermaNET and permAfrost projects it was only possible to purchase expendables (such as batteries, tape, etc.) and change or optimize previously established MTD sites at HLC, DOE or WEI. By the end of December 2012 27 MTD sites with 56 temperature sensors for ground temperature monitoring were operating at the three study areas. At 14 sites 1-channel loggers have been used,

Figure 7: Two photographs of the RDC system at HLC taking daily images from the rooting zone of the rock glacier

at further 13 sites 3-channel loggers were installed (Table 1).

In addition to the three main study areas above, MTDs for monitoring ground surface, near ground surface and air temperature were maintained at additional sites in the Hohe Tauern Range (Pasterze Glacier, Fallbichl-Schareck, Hochtor Pass, Hintereggen Valley, and Kögele Cirque). These activities were not funded within permAfrost. Figure 6 depicts the topographical situations and the locations of the MTDs at HLC, WEI and DOE. Furthermore, the situations for the two study areas Kögele Cirque (KC) – located next to HLC – and Pasterze Glacier (PAG) are indicated in this figure as complementary information.

3.3.3 Monitoring of rooting zone processes using remote digital cameras (RDC)

Two automatic remote digital cameras (RDC) were maintained at the two sites HLC and DOE in order to take daily images of the rooting zones of the two rock glaciers. In the rooting zone snow cover conditions (snow cover duration, melt-out date, avalanches) and mass movement events are of particular interest. The RDC system was a self-developed product during the ALPCHANGE project. The RDC consists of a standard digital camera (Nikon Coolpix 4300), a timer control unit (DigiSnap 2000) and a weatherproof case all mounted on a 1.5 m high steel pole and power supplied by solar panel connected to a storage battery.

The RDC system at HLC was installed on the ridge between HLC and KC at 2770 m a. s. l. in mid September 2006 (Fig. 7). The one at DOE was installed in early September 2006 at a small rock hammock overlooking the rock glacier at an elevation of 2630 m a. s. l.. During the permAfrost project period, RDC data at HLC were collected continuously during the period 19.08.2010 to 15.07.2012 (697 daily images). At DOE the situation is quite different with shorter data availability during the two periods 17.08.2010 to 9.12.2010 (116 images) and 16.08.2011 to 14.2.2012 (183 images). Reason for the failure of the cameras might be technical problems with electronic parts caused by the harsh climatic conditions.

4 Results

4.1 3D-kinematics of rock glaciers

4.1.1 Annual geodetic measurements

All dates of geodetic measurement for the three rock glaciers are listed in Table 2. The reference epoch for comparison is 2009. The table clearly shows that the measurements were carried out almost at the same dates as during the other measurement years with a temporal deviation of only a few days.

In the following, the main results obtained for the three rock glaciers will be presented briefly. Maximum flow velocities obtained at all three rock glaciers are presented in Table 3. The maximum flow velocity is a highly characteristic parameter for rock glacier flow and it can be beneficially used in rock glacier movement analysis (Kellerer-Pirklbauer and Kaufmann 2012). Selected results of horizontal displacement are depicted in Figures 8 to 10 (see also Kaufmann 2013a-c).

Table 2: Dates of geodetic measurements at DOE, HLC and WEI

Rock glacier	2009	2010	2011	2012
DOE	August, 18	August, 17	August, 16	August, 14
HLC	August, 21	August, 21	August, 20	August, 18
WEI	August, 22	August, 20	August, 19	August, 17

Table 3: Maximum flow velocities measured at DOE, HLC and WEI. Observation points are listed within brackets

Rock glacier	2008–2009	2009–2010	2010–2011	2011–2012
DOE	39.7 cm / a (15)	41.7 cm / a (15)	43.1 cm / a (15)	44.5 cm / a (15)
HLC	1.75 m / a (23)	2.43 m / a (23)	2.94 m / a (23)	3.41 m / a (25)
WEI	7.0 cm / a (14)	10.1 cm / a (14)	10.7 cm / a (14)	13.1 cm / a (16)

Flow rates at HLC were exceptionally high throughout the whole monitoring period 1999 to 2012 (Fig. 11). Maximum values were measured for the last measurement year 2011 to 2012. These high flow rates can be most probably explained by the downwasting of large rock masses at the frontal slope. The rock glacier is moving over a terrain ridge into steeper terrain. This geomorphic process is associated with a marked disintegration of the rock glacier surface and the development of surface ruptures (see Fig. 13).

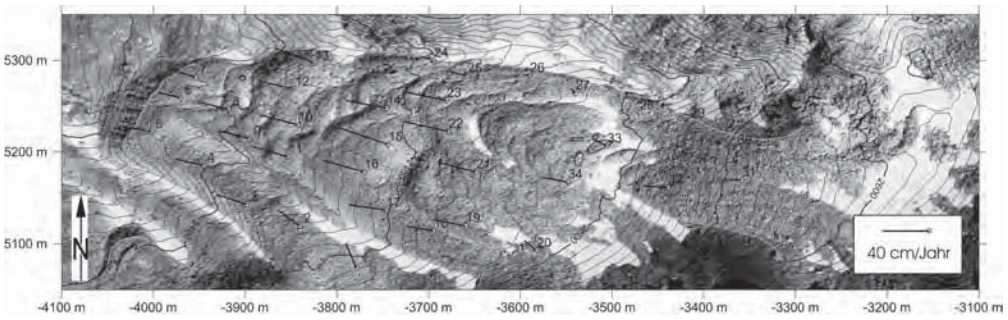

Figure 8: 2D flow vectors at DOE for the time period 2011 to 2012. A maximum flow velocity of 44.5 cm/a was measured at point 15. The total number of observation points on the rock glacier is 109: 34 stabilized points (see this Figure and Figure 2) and 75 paint-marked points.

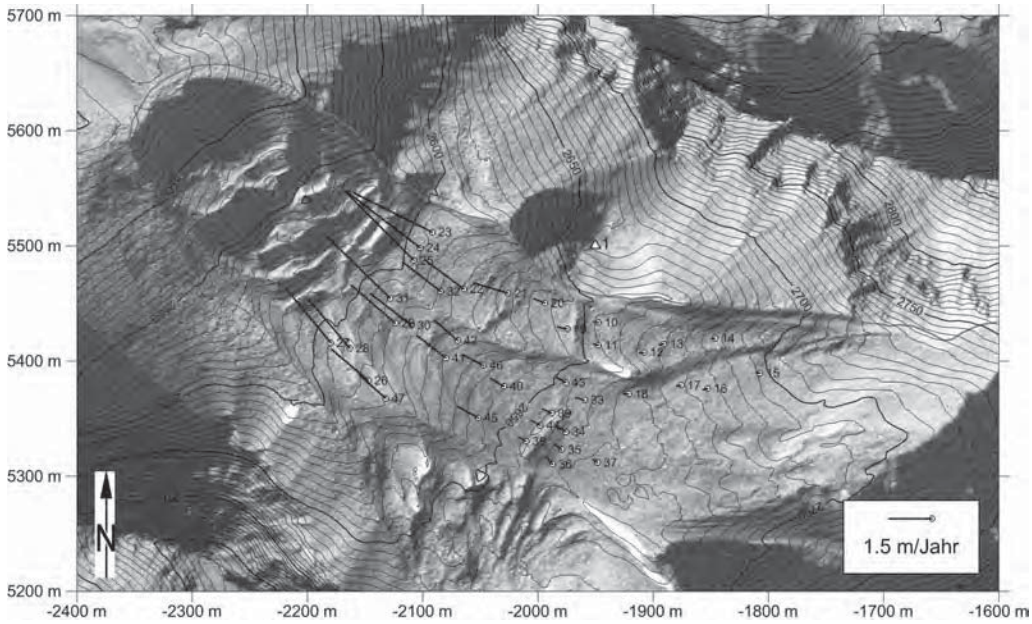

Figure 9: 2D flow vectors at HLC for the time period 2011 to 2012. A maximum flow velocity of 3.41 m/a was measured at point 25. The total number of observation points on the rock glacier is 38 (see Fig. 2)

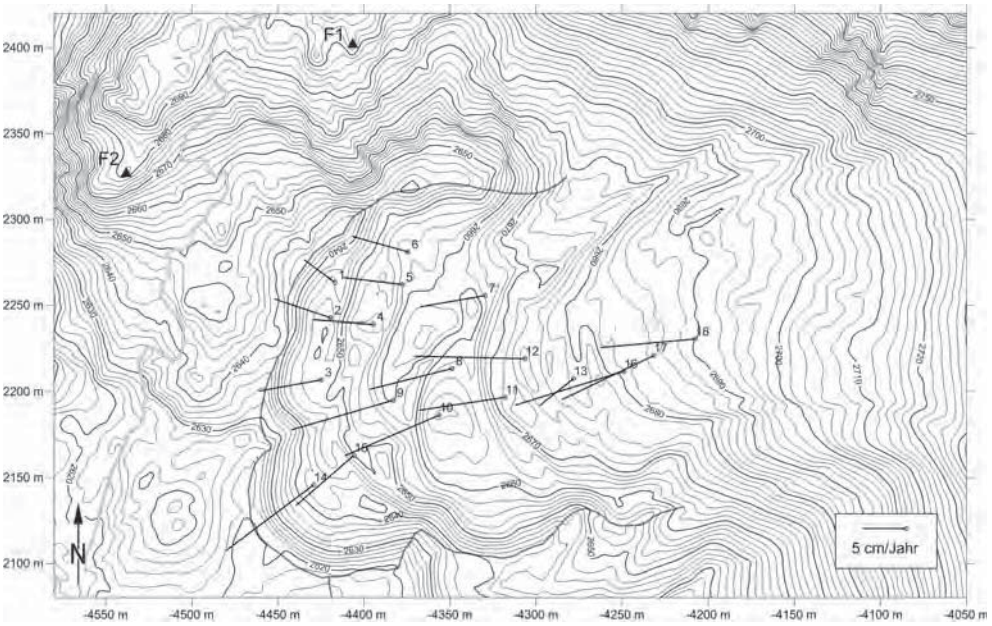

Figure 10: 2D flow vectors at WEI for the time period 2011–2012. A maximum flow velocity of 13.1 cm/a was measured at point 16. The total number of observation points on the rock glacier is 18 (see Fig. 2)

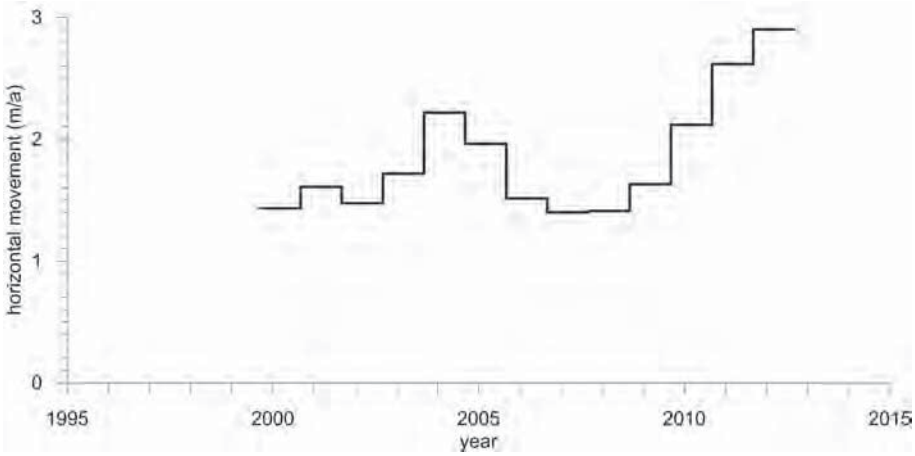

Figure 11: Mean annual horizontal movement of the 6 marked points (23–25, 27, 28, 31) for the time period 1999 to 2012. All 6 points are located at the lower, faster part of the rock glacier HLC

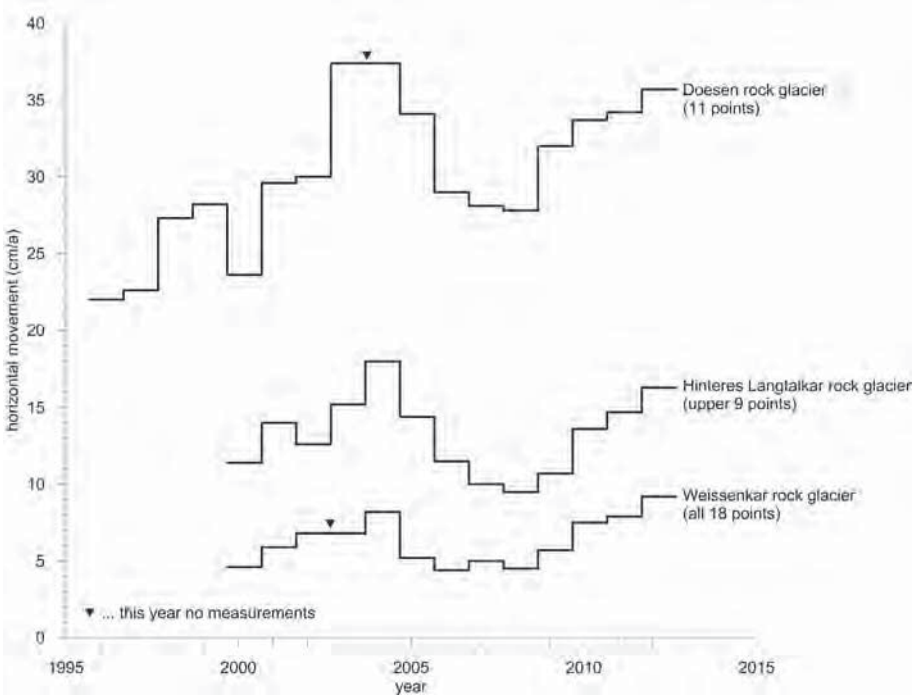

Figure 12: Comparison of the mean annual flow velocities obtained at DOE, HLC and WEI. 11 points at DOE: 10–17, and 21–23; 9 points at HLC: 10–17 and 37 (all points are from the upper part of the rock glacier which is substantially slower compared to the lower part; see Figure 11); all 18 points at WEI.

Figure 13: This figure shows a temporally mixed stereogram of HLC at 80 cm ground sampling distance: a) Google Maps, epoch 2002, b) Microsoft Bing Maps, epoch as at 2006.

Figure 12 shows the temporal change of the mean annual flow velocity for each of the three rock glaciers for the available geodetic data sets. Most interestingly the three curves shown suggest a high correlation of the flow velocities measured. Acceleration and deceleration, respectively, observed at the three rock glaciers are to a high degree synchronous. A possible explanation for this phenomenon give Kellerer-Pirklbauer and Kaufmann (2012). We conclude that climate parameters control to a certain extent rock glacier flow and particularly relative changes in flow velocities.

4.1.2 Photogrammetric surface deformation measurement

High-resolution orthoimages of Google Maps and Microsoft Bing Maps covering HLC date from 18.9.2002 and 21.9.2006 (Fig. 13). Displacement vectors were computed following the procedure of Kaufmann (2010). Based on this information a colour-coded velocity map was generated (Fig. 14). A detailed accuracy analysis of the results obtained and further technical information on the analyses is given in Kaufmann (2012).

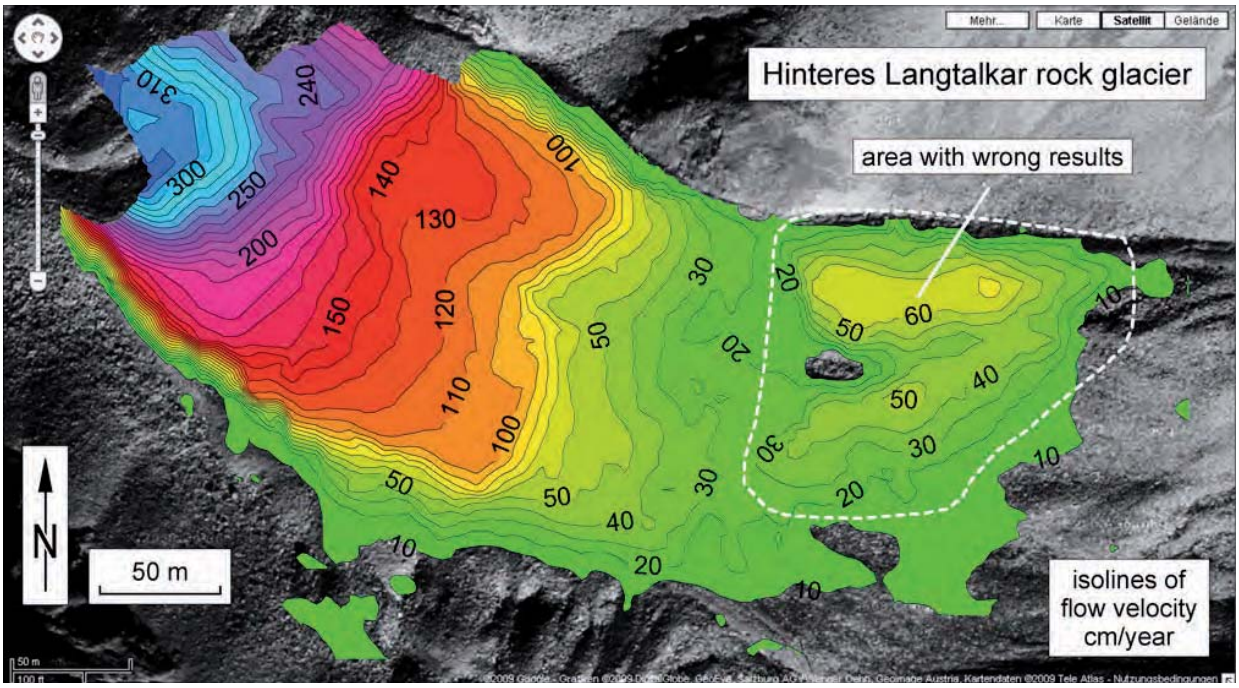

Figure 14: Isolines of mean annual horizontal flow velocity of HLK derived from image data of Google Maps (epoch 2002) and Microsoft Bing Maps (epoch 2006)

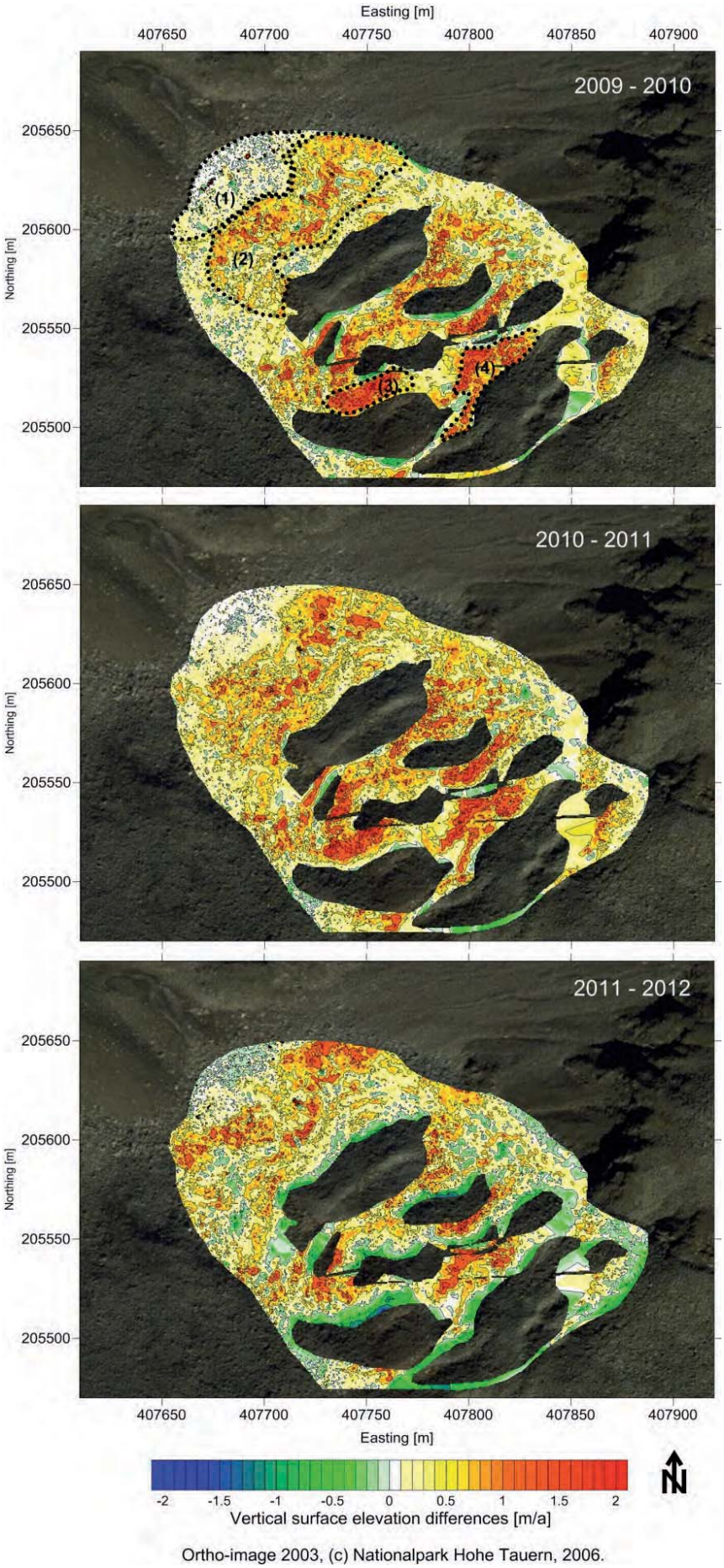

Figure 15: Mean annual vertical surface elevation differences of rock glacier HLC at the epochs 2009 to 2010, 2010 to 2011, and 2011 to 2012. In epoch 2009 to 2010 the delineation of distinct patterns of mean annual vertical surface elevation differences are shown exemplarily and are indicated with the codes (1) to (4)

4.1.3 Surface deformation measurements from Terrestrial Laserscanning

TLS measurements at the rock glacier HLK were carried out on 6.8.2009, 15.9.2010, 25.8.2011, and 1.8.2012. The accuracies of registration of each single point cloud are in the order of ± 2.0 cm considering at least five tie points. In this analysis simple elevation differences of DTMs of each epoch were calculated. Therefore all results do not represent displacement vectors in a strict sense than a vertical change of a pixel in a positive (surface lifting) or negative (surface decline) direction which is below termed as vertical surface dynamics.

Table 4 presents mean vertical surface elevation changes for different areas at the front of the rock glacier HLC based on the TLS campaigns. Mean vertical surface elevation changes over the entire rock glacier tongue (extent see Fig. 15) are in the range of 39 to 45 cm / a with a peak at the epoch 2010 / 11. For all three epochs, four areas with similar patterns of vertical surface dynamics can be differentiated. The four similar areas are exemplarily delineated for the epoch 2009 to 2010 shown in Figure 15.

1. The lowest part of the front of the rock glacier HLC is quite stable in terms of small vertical surface elevation changes. This part is characterized by accumulated loose debris transported down from the adjacent moving part uphill (Table 4 "(1)").
2. Adjacent uphill, a large area with high vertical movement rates (> 0.57 m / a at all epochs) can be detected. This vertical surface lifting can be equalized – in terms of geomorphological process interpretation – with an intense downslope movement (Table 4 "(2)").
3. The upper part of the rock glacier front can be differentiated in a left and central part with high positive vertical movement rates (> 0.80 m / a at all epochs, Table 4 "(3)" as well as "(4)").

Table 4: Mean vertical surface elevation changes (-> dynamics) from TLS at the entire front lobe and the four distinct parts of HLC from TLS.

Rock glacier HLC	2009–2010	2010–2011	2011–2012
Mean	0.39 m / a	0.47 m / a	0.39 m / a
Area (1)	0.08 m / a	0.11 m / a	0.13 m / a
Area (2)	0.64 m / a	0.65 m / a	0.57 m / a
Area (3)	1.12 m / a	0.80 m / a	0.80 m / a
Area (4)	0.98 m / a	0.97 m / a	0.79 m / a

4.2 Internal structure of rock glaciers based on geophysical measurements

Geophysical field work at the three rock glaciers was carried out during the period 17.8.2011 to 6.9.2011. At HLC two geoelectrical profiles and 148 VLF points were measured. At WEI three geoelectrical profiles and 126 VLF points were measured. Finally, at DOE four geoelectrical profiles (although only three successfully) and 122 VLF points were measured. The locations of the profiles are indicated in Figure 2. Results of VLF and from geoelectrical profiles do coincide in terms of high and low resistivity values but cannot be compared directly. Although results of VLF seem to be coarse in terms of resolution, results seem to distinguish areas without permafrost from ice rich areas.

4.2.1 Indicators for internal structure at HLC

Due to very unfavorable terrain conditions and time consuming campaigns only areas between the geoelectric sections were measured with 148 VLF-points at the rock glacier HLC. VLF-results show a shift of resistivity from NE to SW with a low resistivity anomaly in NW and a high resistivity anomaly in SE and therefore a change in the inner structure of the rock glacier (Fig. 16, left).

The two geoelectrical profiles at HLC (Fig. 2 for locations) are briefly described. Profile HLC-P1 (50 electrodes, length 490 m) started from bedrock (BR, "profile-meter" PM1–60 and from PM460 on, overlain by a shallow debris cover), followed by a slope section of blocky debris (BD, depth 10 m, PM60–PM140). Under this scree slope low values of resistivity were measured which can be interpreted as jointed bedrock allowing groundwater flow and hence reduced resistivity values. Adjacent (PM140–PM220) measurements suggest a rather dry bedrock area. The section between PM215 and PM460 comprises ice rich areas which can be indicated as the main rock glacier body. Resistivity values suggest two homogeneous units whereas the section with significantly lower values covers PM215–PM280 with

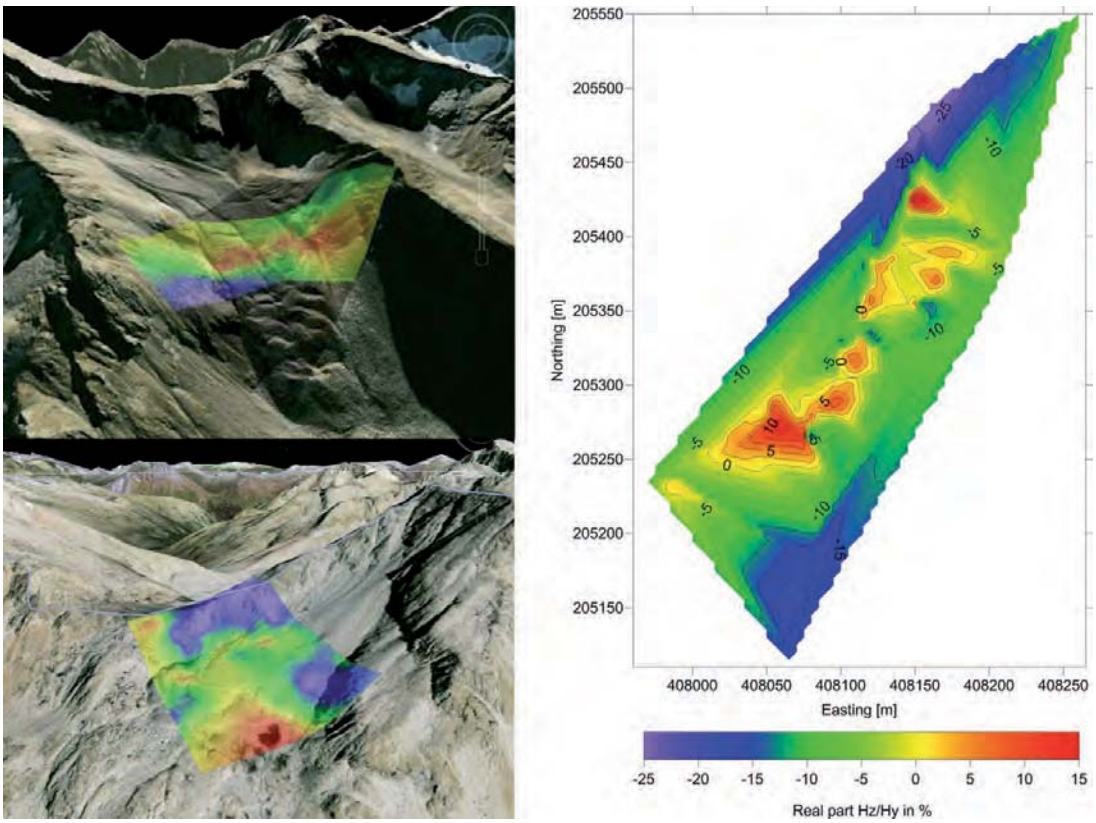

Figure 16: Left – 3D visualization of interpolated VLF-data at rock glacier HLC (left-top) and the rock glacier WEI (left-bottom). Right – Isolines of interpolated VLF-data for HLC. Legend is valid for all three sub-figures

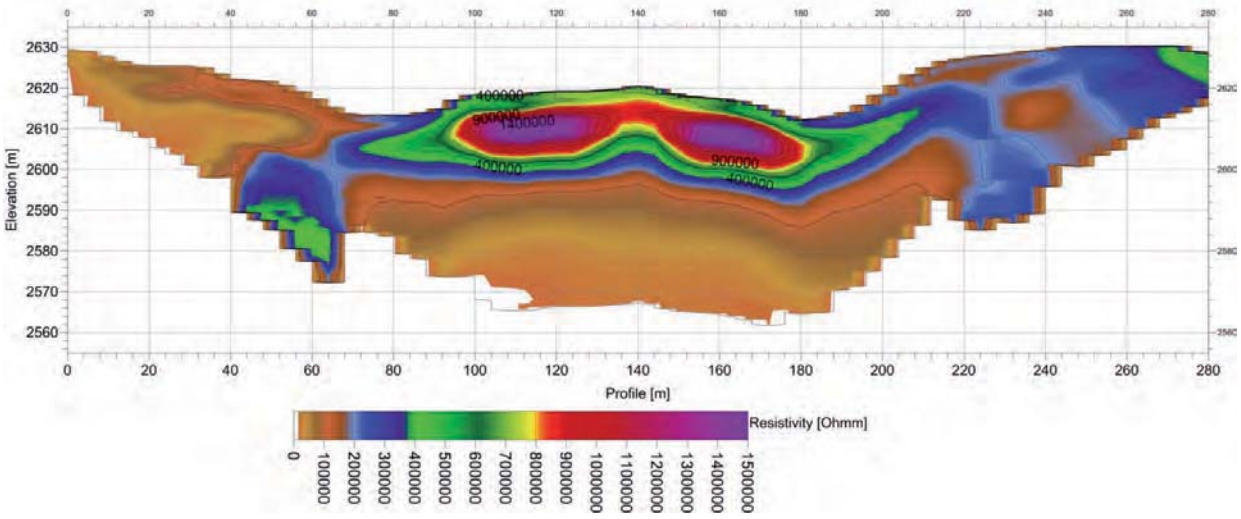

Figure 17: Results at the geoelectrical profile P2 and the rock glacier HLC

depths up to 20 m as well as the section with significantly higher values from PM280–PM365 with depths up to 15 m. Between PM200 and PM380 a layer of very low resistivity values was measured in depths of > 40 m.

Profile HLC-P2 (30 electrodes, length 290 m) is characterized by similar measurement values as in Profile HLC-P1, although areas with very high resistivity – compared to HLC-P1 – were measured too (Fig. 17). The beginning of the profile was set on bedrock as at HLC-P1 (until PM60), which is also overlain by a shallow debris cover (5 m). The rock glacier body itself begins at PM60 with a significant increase of resistivity values. From PM70 very high resistivities with depths to 20 m were measured until PM190 and down to 10 m until PM220.

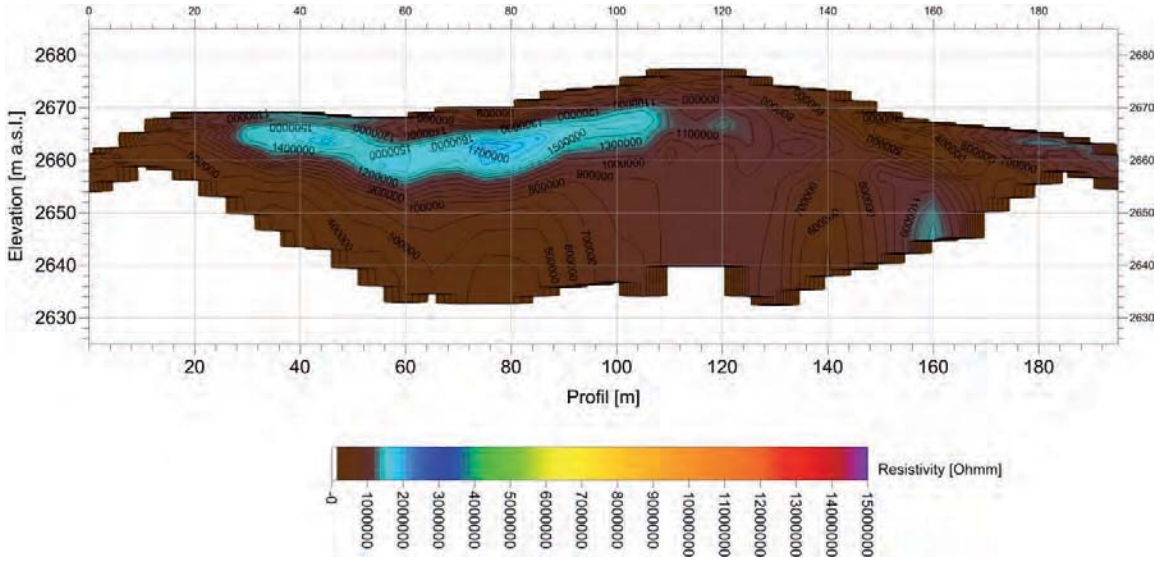

Figure 18: Results at the geoelectrical profile P3 and the rock glacier WEI

4.2.2 Indicators for internal structure at WEI

At rock glacier WEI three geoelectric profiles (Fig. 2) and 126 VLF points were measured. Generally it can be stated that all resistivity measurements are one magnitude higher than measurements on rock glacier HLC.

Profile WEI-P1 (30 electrodes, length 290 m, alignment: N–S): WEI-P1 transects the rock glacier transversally. High resistivities are detectable beginning with PM20 consistently until PM145, thicknesses vary from 10 m at the N of the rock glacier to 15 m at left margin in the S of WEI. Thickness of the active layer is about 4–5 m.

Profile WEI-P2 (20 electrodes, length 190 m, alignment: W–E, intersected WEI-P1 orthogonal at PM100): The results from longitudinal profile WEI-P2 correspond well with WEI-P1 in the transitionszone. At PM45 resistivity values increase significantly indicating an ice-rich area with a thickness of 20 m until PM150.

Profile WEI-P3 (20 of 23 electrodes usable, length 220 m, at rock glacier front): This section shows evidences of ice-rich substrate beginning with PM30 until PM110 under active layer of 4 to 6 m (Fig. 18). At this part of the rock glacier ice rich substrate – hence permafrost – seems to occur as a lens. This seems feasible considering a radiation favoring location (W-facing slope), the relative low elevation and the relative low movement rates as revealed by the annual geodetic campaigns.

4.2.3 Indicators for internal structure at DOE

At DOE four geoelectrical profiles were measured originally although only three successfully (Fig. 2) because of problems with conductivity occurring at profile DOE-P1 during the field campaign. The results from the remaining three profiles are briefly described.

Profile DOE-P2: The profile transects the upper part of the rock glacier longitudinally / downslope (30 electrodes, 5 m distance = length 145 m, alignment: E–W). From PM40 on high resistivities at a depth of 5 m indicate ice-rich substrate. This presumably solid permafrost body of at least 10 to 15 m thickness – in horizontal as well as in vertical extent – distinctly ends at PM115.

Profile DOE-P3 (Fig. 19): The profile follows a ridge at the orographic left part of the lower rock glacier area (34 electrodes, 6 m distance = length 198 m, alignment: SE–NW). At this longitudinal profile evidences of a permafrost body start at PM8 with high resistivities in a depth of 4 m and a thickness of 4 to 5 m to PM20 followed by low resistivities until PM35.

From PM35 on high resistivities in a depth of 3 to 5 m with a thickness of 12 to 15 m, continuing until PM160. The near surface sediments consisting of large blocks and fine grained substrate show thicknesses of 4 to 5 m, the thickness of ice-rich areas (permafrost body) shows continuous thicknesses of 12 to 15 m.

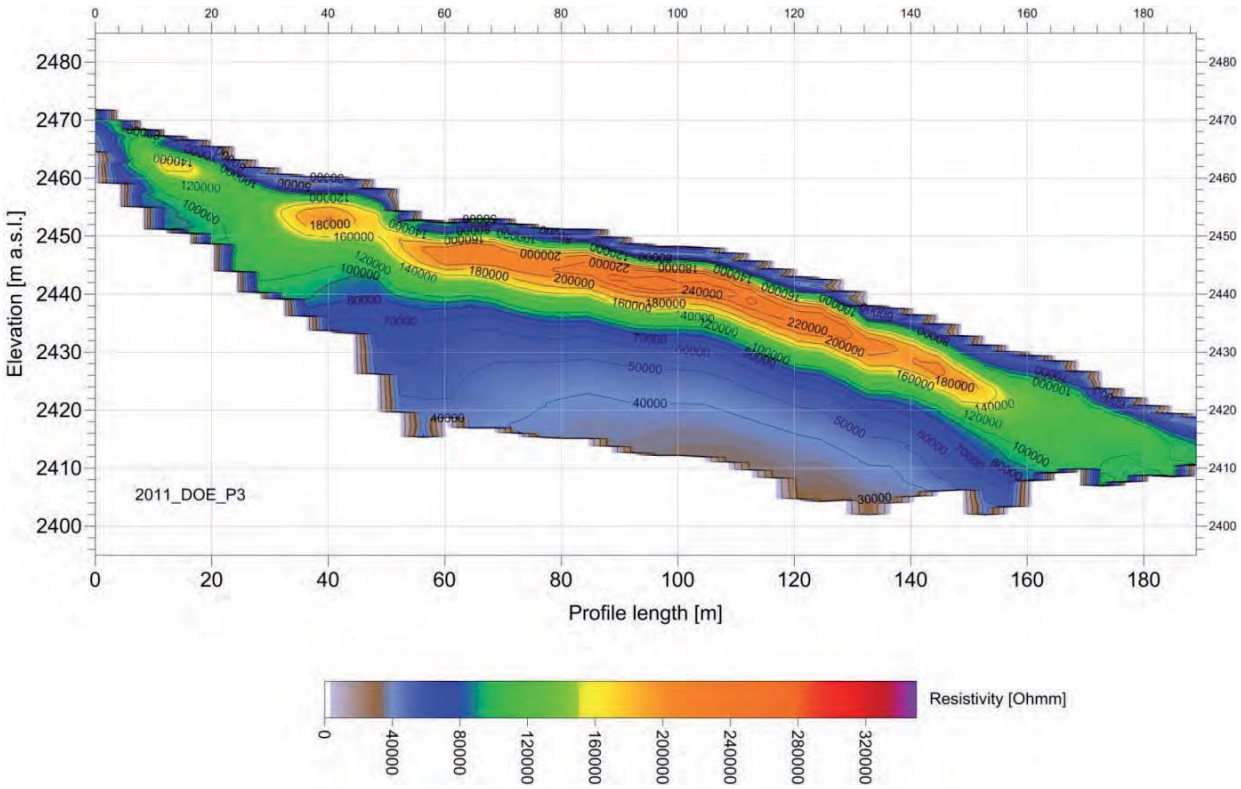

Figure 19: Results at the geoelectrical profile P3 and the rock glacier DOE

Profile DOE-P4: The profile follows the orographic left (southern) margin of the rock glacier body. (40 electrodes, 5 m distance = length 195 m, alignment: SE–NW). At this profile only marginal evidences of permafrost with thicknesses of ca. 8 m between PM35 and PM75 were detected (lowest elevation: 2410 m a.s.l.). Due to the setting on the left margin of the rock glacier it clearly shows a transition of a permafrost area to a permafrost-free area.

4.3 Permafrost and climate monitoring

4.3.1 Meteorological data at DOE and HLC

Table 5 lists the collected meteorological data with data gaps and periods of field campaigns between 2010 and 2012. The data gaps are related to the harsh environmental conditions and animals damaging sensors or cables. When possible, sensors were repaired or changed during the field campaigns. Some details for example: One anchoring wire rope at the AWS HLC was destroyed presumably by a lightning stroke in 2009 to 2010 and repaired in 2010 and further improved in 2011. At the DOE AWS site, the sensor collecting relative humidity and air temperature was destroyed during the measurement year 2010 to 2011. Therefore, a new combined relative humidity-air temperature sensor (EE08, EE Electronics, Austria) was installed in 2011.

Data from the two AWS sites were for instance used in the analyses for the publication regarding the relationship between rock glacier velocity and climate parameters thereby analysing the three different rock glaciers (Kellerer-Pirklbauer & Kaufmann 2012). In this work climate data were combined with ground temperature data and rock glacier velocity data. By correlating rock glacier velocity with different climatic parameters (air temperature, snow depth, ground surface temperature and ground temperature at 1 m depth and derivatives of them) it was shown that the relationships are complex and only in few cases statistically significant. Most of the correlating pairs of variables support the observation that warmer air temperatures, warmer ground surface temperatures, and warmer ground temperatures at 1 m depth (or derivatives of the three parameters) favour faster rock glacier movement and therefore rock glacier acceleration. The most striking problem during the analysis were short time series in particular of ground temperature (surface and at one meter

Table 5: Data series collected from the two automatic weather stations (AWS) at the two study areas DOE and HLC during the permAfrost-WP4000 project period starting on 1 June 2010. Periods of field campaigns to the study areas DOE and HLC including WEI are indicated in the last row

Station	Data series	Comment	Field campaigns
AWS-DOE	010610-150511	Partly data available; no data for air humidity	16.–18.08.2010 15.–17.08.2011 17.–18.10.2011 19.–21.08.2012 24.–25.09.2012
	150511-160811	Partly data available; no data for air humidity and air temperature	
	160811-090212	Data series completely available, no problems	
	100212-080712	Partly data available; no data for global radiation	
	080712-200812	Partly data available; no data for global radiation and maximum wind speed	
AWS-HLC	010610-150910	No data available; problem with lightning stroke effects	18.–21.08.2010 15.–16.09.2010 17.–20.08.2011 21.–25.08.2012
	160910-060112	Data series completely available, no problems	
	060112-220812	Partly data; sensor for air temperature and humidity malfunctioned due to cable destruction	

depth). For details on these analyses refer to Kellerer-Pirklbauer & Kaufmann (2012).

4.3.2 Ground temperature data at HLC, WEI and DOE

In general, the MTDs worked quite well at all three study sites and no major problems were faced during the field campaigns. Results presented in Kellerer-Pirklbauer (2013) clearly revealed ground surface warming at most MTD sites since 2006. Over the last years warming was stronger in the western part of the national park (study areas HLC and WEI) in relation to the eastern part (DOE). This warming generally influences all elevations above ca. 2 000 m a. s. l., all slope inclinations, all aspects and seems to be unrelated to winter snow cover conditions at the MTD sites as indicated by the analyses. Figure 20 shows the trend results for the 27 MTD sites in our three main study areas based on all available data for each site using linear regression. Furthermore, Figure 21 shows two examples of temperature evolution (based on mean daily data) since the beginning of the measurements: one example reveals a warming trend (HLC-UP-S), the second example reveals no trend at all (DOV-UP-S). Both sites are permafrost-sites as indicated by the base temperature of the winter snow cover (BTS) in late winter at HLC-UP-S (Haeberli 1973) for HLC-UP-S or the low mean annual ground surface temperature for DOV-UP-S. For details and other analyses based on the MTD-data refer to Kellerer-Pirklbauer (2013).

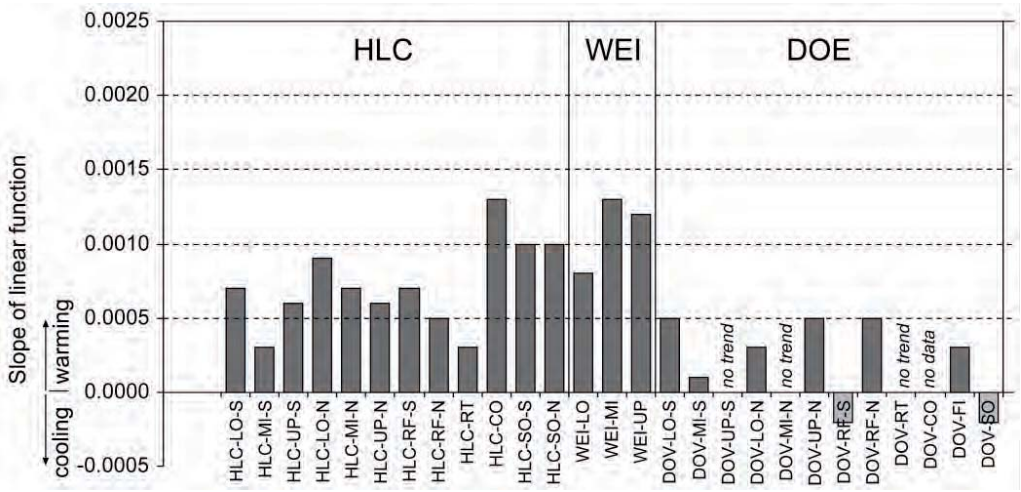

Figure 20: Slope of linear function for ground surface temperature using linear regression for all MTD-sites at the three study areas WEI, HLC and DOE. The calculated trends are based on all available daily mean data per site. In most cases data series start in 2006

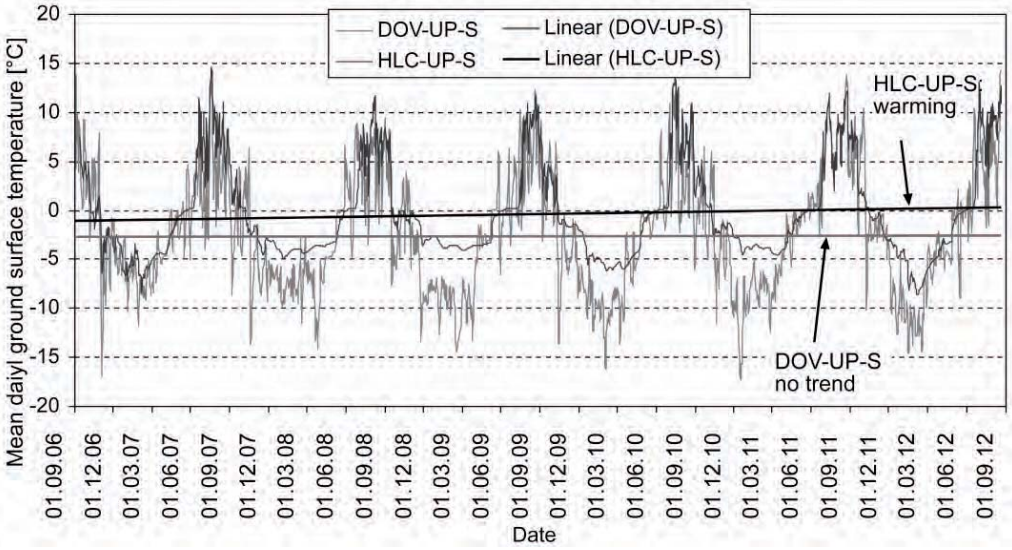

Figure 21: Mean ground surface temperature evolution at two MTD sites. One example indicates no trend and hence neither warming nor cooling of the surface at all (DOV-UP-S), a second example indicates a clear warming trend (HLC-UP-S)

4.3.3 Optical monitoring based on the RDC data at HLC and DOE

The RDC system at HLC has been running more stable compared to DOE with shorter data gaps. Particularly the good data quality at HLC allowed a detailed analysis which were analysed primarily within the framework of a master thesis (Rieckh 2011) and presented at different conferences (Kellerer-Pirklbauer et al. 2010, Rieckh et al. 2011). Figure 22 exemplarily shows snow cover duration maps for the hydrological years 2006 to 2007 and 2007 to 2008 in the north-eastern rooting zone of the rock glacier HLC. Note the distinct differences in the duration but the general similarity in the pattern. The duration difference is related to the snow-poor conditions during the first year and rather normal snow conditions during the second year (as can be judged by data comparison with snow data from the neighbouring meteorological observatory at Mt. Hoher Sonnblick).

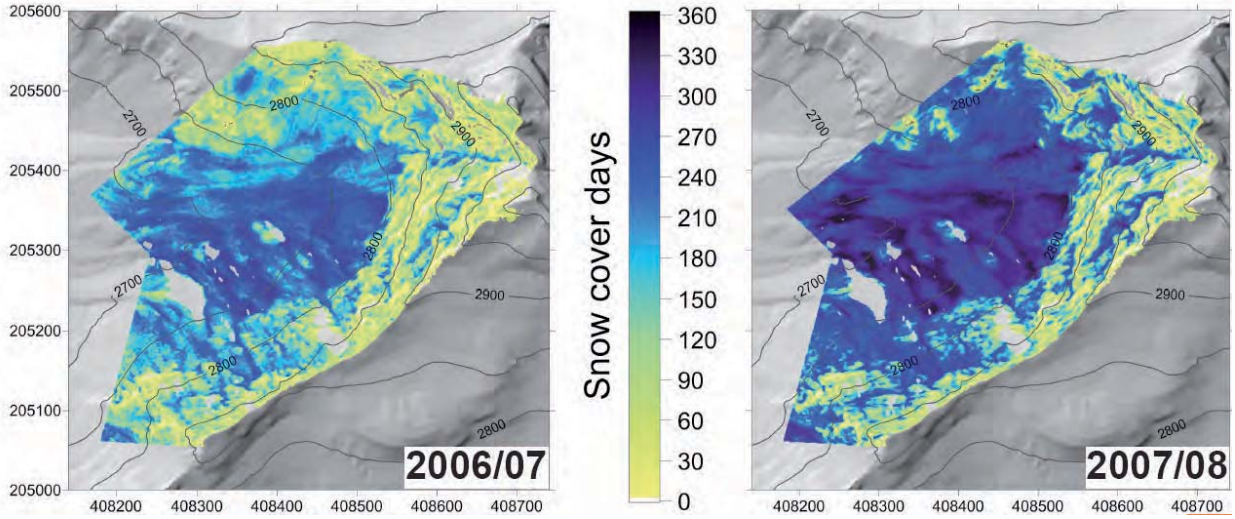

Figure 22: Snow cover duration maps for two years at the rooting zone of the Hinteres Langtalkar Rock Glacier based on daily optical data from the RDC system installed above the area of interest. For analytical approach and technical details see Rieckh (2011)

5 Synthesis of results

5.1 Synthesis for WEI

Rock glacier WEI is the slowest moving one of the three studied rock glaciers. This rock glacier is also different to the other two rock glaciers because of the radiation exposed site, the relatively warm ground surface temperatures measured at three sites at the rock glacier surface and the results for the geophysical measurements indicating a discontinuous permafrost body in the rock glacier sediments possibly indicative for a tendency of this rock glacier to turn to climatic inactive (Barsch 1996).

At two of the three MTD sites mean ground surface temperatures are positive during the period 2006 to 2012. In addition to that, all three sites show a clear warming trend during this period (Fig. 21). Furthermore, geoelectrical profiles at the central part of the rock glacier WEI show clear evidence of ice rich substrate under an active layer of 4 to 5 m. The thickness of the permafrost body is assumed to be ca. 15 to 20 m, the transversal extent along the profile WEI1 is expected with ca. 120 m. Therefore ice is very likely along most of the rock glacier. Permafrost in the lowest part of the rock glacier WEI can be expected as marginal and if so only expressed by isolated lenses. This argument is comprehensible considering a radiation favoring location, the rather low elevation and the rather low movement rates as revealed by the annual geodetic campaigns.

5.2 Synthesis for HLC

Rock glacier HLC is very special because of the disintegration processes which started in the mid 1990s causing tearing-apart surface structures. Transversal assemblages of furrows and ridges with very high rate (for rock glaciers at least) at the frontal part and substantially lower rates at the upper-most part determine the appearance of the rock glacier particularly. This peculiarity makes this rock glacier of special interested leading to permafrost-related research at this rock glacier since the 1990s (see Kellerer-Pirklbauer and Kaufmann 2012 for complete references).

The lower part of the rock glacier HLC is characterized by different areas of the vertical surface elevation differences between the epochs with distinct patterns. Disintegration and extensive mass wasting especially at the very front of the rock glacier still proceeds making in situ field work also very difficult and dangerous. Mean values of vertical surface elevation changes at the frontal part are in the range of 40 to 45 cm / a, which is significantly higher than values of 30 to 35 cm / a in the period 2005 to 2008 (Avian et al. 2009). This also coincides with 3D deformation measurements at the middle (Fig. 12) and upper parts (Fig. 14) of the rock glacier HLC. Summarizing it can be stated that different measurements show that the 3D kinematics of the rock glacier increase since the epoch 2007 to 2008 after a period of decrease since a first peak at the epoch 2004 to 2005. Furthermore, ground surface temperatures clearly indicate a warming trend since 2006 which is in agreement with the possible effects of ground warming explained above.

DC-resistivity measurements have been carried out just above the upper part of the TLS measurements and in between the lowest parts of geodetic surveys. Results show that permafrost is very likely in a depth of 3 to 5 m with thicknesses of about 20 m with an extent of 120 m along the profile. As mentioned above displacement rates increase from the epoch 2008 / 2009 to 2011 / 2012. All measurements at the rock glacier HLC show prolonging very high movement rates at the front of the rock glacier and thus of strain related processes such as disintegration and frequent mass wasting at the frontal zone.

5.3 Synthesis for DOE

The rock glacier DOE shows surface movement rates which numerically are in between the rates of WEI und HLC (lower part). In contrast to HLC this rock glacier does not have any crevasse-like structures due to strain or mass-wasting. DOE is rather homogenous in its movement pattern (Fig. 8) and can be regarded as a “standard” rock glacier at that size. Interestingly, mean ground temperatures at the MTD sites are cooler compared to the MTD sites at HLC and WEI. Furthermore, during the last six years no clear trend in ground surface warming or cooling for this rock glacier was detected.

Geoelectrical profiles at the central part of the rock glacier DOE show clear evidence of ice-rich

substrate under an active layer of 4 to 5 m. The thickness of the permafrost body is assumed to be appr. 10 to 15 m evenly along the entire longitudinal profile DOE 3 at the central part of the rock glacier. Profiles at the margin of the rock glacier (P2, P4) show a marginal continuation of ice-rich substrate to the adjacent N-facing slopes which proofs the assumption of ice lenses within these scree slopes.

6 Conclusion and outlook

The annual displacement vectors obtained are highly congruent at each of the three rock glaciers. Flow/creep directions are mostly consistent throughout a longer period of time, i. e. 2 to 3 years. Furthermore and most importantly, the geodetic measurements 2010 to 2012 confirmed once more our working hypothesis that the annual changes of flow velocity at the three rock glaciers are highly correlated with one another due to common, external forces, such as air temperature (see a more detailed analysis in Kellerer-Pirklbauer and Kaufmann, 2012). At Hinteres Langtalkar rock glacier maximum flow velocities of up to 3.41 m / a were measured, at Dösen 44.5 cm / a, and at Weissenkar rock glacier 13.1 cm / a, respectively.

In order to better study the influence of climate change on rock glacier movement it is necessary to continue the long-term geometric monitoring at least at this time scale, i. e. a one year interval. However, to better address geomorphic process understanding at rock glaciers the authors propose the installation of a continuous geometric monitoring system which is capable of providing daily flow / creep rates. This could be accomplished by a wireless network of Real-time Kinematic (RTK) low-cost Global Navigation Satellite System (GNSS) receivers. Such a system should then be augmented by other important sensors, such as temperature loggers or hydraulic pressure gauges.

Furthermore it is evidently important to continue and extent the long-term thermal monitoring at these three rock glacier sites, but also other "key-sites" in the Austrian Alps. These sites should be well distributed in different permafrost environments from Western to Central and Eastern Austria. Furthermore, this distribution should consider permafrost sites in the north (Northern Calcareous Alps), in the centre (Central Alps such as e. g. Hohe Tauern Range) as well as the south (Southern Calcareous Alps) of the Austrian Alps. As indicated by our measurements, temperature trends at MTD sites indicate warming in the Schober and Glockner Mountains whereas in the Ankogel Mountains to the east, no clear trends were revealed indicating more stable (permafrost-) conditions in this mountain group. However, obviously longer time series of ground temperature would be certainly helpful to clearer detect such signals.

Geophysical surveys delivered satisfying results although – as methodologically had to be expected – absolute values were not comparable between each rock glacier. Generally differences in resistivity-measurements within the permafrost body can be explained by changes in temperature, thickness, fine grained fraction, and/or stress. Furthermore usage of very low frequency (VLF) measurements showed its feasibility for determining ice / no-ice areas within permafrost areas with very promising results for overview purposes. Improved methodology and implementation of VLF is of great interest for upcoming analyses in high mountain permafrost areas.

Summarizing, this research report clearly illustrates that the combination of the different methods enabled the generation of valuable research results. However, data processing is partly still ongoing and more research results will be published in the future. Furthermore, usage of further methods and instrumentations e. g. continuous movement monitoring, boreholes in permafrost, and other geophysical methods would be very helpful to improve the understanding of rock glaciers.

7 Acknowledgements

This research project was carried out within the project "permAfrost – Austrian Permafrost Research Initiative" funded by the Austrian Academy of Sciences. Furthermore, relevant data were collected earlier within the two projects "ALPCHANGE – Climate Change and Impacts in Southern Austrian Alpine Regions" financed by the Austrian Science Fund (FWF) through project no. FWF P18304-N10 as well as "PermaNET – Permafrost long-term monitoring network". PermaNET is part of the European

Territorial Cooperation and co-funded by the European Regional Development Fund (ERDF) in the scope of the Alpine Space Programme. Furthermore, we are very thankful to Dr. Devrim Akca for providing the software LS3D (ETH-Zurich).

Unfortunately, Dr. Erich Niesner deceased during the project period. He was a sincere colleague with splendid ideas allowing fruitful discussions. In order to honor his valuable work during the years but also to honor him as a person, we dedicate this project report in memory of Erich.

8 References

Akca, D., 2010. Co-registration of surfaces by 3D Least Squares matching. Photogrammetric Engineering and Remote Sensing, 76 (3): 307–318.

Avian, M., Lieb, G.K. and Kaufmann, V., 2005: Recent and Holocene dynamics of a rock glacier system – the example of Langtalkar (Central Alps, Austria). Norsk Geografisk Tidsskrift – Norwegian Journal of Geography, 59: 1–8.

Avian M., Kellerer-Pirklbauer A. and Bauer A. 2008. Remote Sensing Data for Monitoring Periglacial Processes in Permafrost Areas: Terrestrial Laser Scanning at the Rock Glacier Hinteres Langtalkar, Austria. Proceedings of the Ninth International Conference on Permafrost (NICOP), University of Alaska, Fairbanks, USA, June – July 2008: 77–82.

Avian, M., Kellerer-Pirklbauer, A., and Bauer, A., 2009. LiDAR for monitoring mass movements in permafrost environments at the cirque Hinteres Langtal, Austria, between 2000 and 2008, Nat.Hazards Earth Syst. Sci., 9: 1087–1094. doi:10.5194/nhess-9-1087-2009.

Avian M., and Kellerer-Pirklbauer A., 2012. Modelling of potential permafrost distribution during the Younger Dryas, the Little Ice Age and at present in the Reisseck Mountains, Hohe Tauern Range, Austria. Austrian Journal of Earth Sciences, 105 (1): 140–153.

Baltsavias, E. P., 1999. A comparison between photogrammetry and laserscanning ISPRS Journal of Photogrammetry and Remote Sensing, 54 (2–3): 83–94.

Barsch, D. 1996. Rockglaciers. Indicators for the Present and Former Geoecology in High Mountain Environments. Springer Series in Physical Environment 16. Springer-Verlag, Berlin, 331 pp.

Bauer, A., Paar, G., and Kaufmann, V., 2003. Terrestrial laser scanning for rock glacier monitoring, in: Proceedings of the 8th International Permafrost Conference, edited by: Phillips M., Springman S.M., and Arenson L.U., Zurich, Balkema 1: 55–60, 2003.

Berthling, I., 2011. Beyond confusion: rock glaciers as cryo-conditioned landforms. Geomorphology, 131: 98–106.

Bodin, X., and Schoeneich, P., 2008. High-resolution DEM extraction from terrestrial LIDAR topometry and surface kinematics of the creeping alpine permafrost: The Laurichard rock glacier case study (Southern French Alps), In: Kane, D.L., and Hinkel, K.M., (eds.), Ninth International Conference on Permafrost. Institute of Northern Engineering, University of Alaska at Fairbanks, 1: 137–142.

Boeckli, L., Brenning, A., Gruber, S. and Noetzli J. 2012. A statistical permafrost distribution model for the European Alps, The Cryosphere, 6: 125–140. doi:10.5194/tc-6-125-2012

Delaloye, R., Perruchoud, E., Avian, M., Kaufmann, V., Bodin, X., Hausmann, H., Ikeda, A., Kääb, A., Kellerer-Pirklbauer, Krainer, K., Lambiel, Ch., Mihajlovic, D., Staub, B., Roer, I. and Thibert, E., 2008. Recent interannual variations of rock glacier creep in the European Alps. In: D.L. Kane and K.M. Hinkel (eds.), Proceedings of the Ninth International Conference on Permafrost (NICOP), University of Alaska, Fairbanks, USA: 343–348.

French, H.M., 1996. The Periglacial Environment - 2nd Edition. Harlow, Longman, 341 p.

Haeberli , W., 1973. Die Basis-Temperatur der winterlichen Schneedecke als möglicher Indikator für die Verbreitung von Permafrost in den Alpen. Zeitschrift für Gletscherkunde und Glazialgeologie, 9 (1-2): 221–227.

Haeberli , W., Guodong, C., Gorbunov, A.P. and Harris, S, 1993. Mountain permafrost and climate change. Permafrost and Periglacial Processes, 4: 165–174.

Haeberli, W., Hallet, B., Arenson, L., Elocin, R., Humlum, O., Kääb, A., Kaufmann, V., Ladanyi, B., Matsuoka, N., Springman, S., and Vonder Muehll, D., 2006. Permafrost creep and rock glacier dynamics. Permafrost and Periglacial Processes, 17: 189–214. DOI: 10.1002/ppp.561

Karous, M. and Hjelt, S.-E., 1977. Determination of apparent current density from VLF measurements. Contribution No. 89, Department of Geophysics, University of Oulu. http://www.cc.oulu.fi/~mpi/Softat/pdfs/KarousHjelt_1977.pdf

Kaufmann, V., 2010. Measurement of surface flow velocity of active rock glaciers using orthophotos of virtual globes. Geographia Technica, Special Issue, Cluj University Press: 68–81.

Kaufmann, V., 2012. Detection and quantification of rock glacier creep using high-resolution orthoimages of virtual globes. Int. Arch. Photogramm. Remote Sens. Spatial Inf. Sci., XXXIX-B5, 517–522, doi:10.5194/isprsarchives-XXXIX-B5-517-2012.

Kaufmann, V., and Ladstädter, R., 2003. Quantitative analysis of rock glacier creep by means of digital photogrammetry using multi-temporal aerial photographs: two case studies in the Austrian Alps. In:

Permafrost. Proceedings of the Eighth International Conference on Permafrost, A.A. Balkema Publishers, 1: 537–541.

Kaufmann, V., Filwarny, J.O., Wisiol, K., Kienast, G., Schuster, V., Reimond, S., and Wilfinger, R., 2012. Leibnitzkopf Rock Glacier (Austrian Alps): Detection of a fast Moving Rock Glacier and Subsequent Meassurement of its Flow Velocity. Proceedings of the Tenth International Conference on Permafrost, Volume 4/1: Extended Abstracts, The Fort Dialog-Iset Publisher, Ekaterinburg, Russia: 259–250.

Kaufmann, V., 2013a. http://www.geoimaging.tugraz.at/viktor.kaufmann/Doesen_Rock_Glacier/index.html

Kaufmann, V., 2013b. http://www.geoimaging.tugraz.at/viktor.kaufmann/Hinteres_Langtalkar_Rock_Glacier.html

Kaufmann, V., 2013c. http://www.geoimaging.tugraz.at/viktor.kaufmann/Weissenkar_Rock_Glacier.html

Kellerer-Pirklbauer, A. 2008: Aspects of glacial, paraglacial and periglacial processes and landforms of the Tauern Range, Austria. Doctoral Thesis, University of Graz, 200 p.

Kellerer-Pirklbauer A., 2013: Ground surface temperature and permafrost evolution in the Hohe Tauern National Park, Austria, between 2006 and 2012: Signals of a warming climate? 5th Symposium for Research in Protected Areas – Conference Volume, 10 to 12 June 2013, Mittersill, Austria, 363–372.

Kellerer-Pirklbauer, A., and Kaufmann, V., 2012. About the relationship between rock glacier velocity and climate parameters in central Austria. Austrian Journal of Earth Sciences 105 (2): 94–112.

Kellerer-Pirklbauer A. and Kaufmann V. in prep. Cryospherical and morphodynamical changes in deglaciating cirques in central Austria and its possible significance for permafrost and rock glacier evolution. Geomorphology.

Kellerer-Pirklbauer A., Bauer A. and Proske H. 2005. Terrestrial laser scanning for glacier monitoring: Glaciation changes of the Gößnitzkees glacier (Schober group, Austria) between 2000 and 2004. Proceedings of the 3rd Symposium of the Hohe Tauern National Park for Research in Protected Areas, Kaprun, Austria, September 2005: 97–106.

Kellerer-Pirklbauer A., Rieckh M. and Avian M. 2010. Snow-cover dynamics monitored by automatic digital photography at the rooting zone of an active rock glacier in the Hinteres Lantal Cirque, Austria. Geophysical Research Abstracts 12: EGU2010-13079.

Kellerer-Pirklbauer A., Lieb G.K. & Kleinferchner H. 2012. A new rock glacier inventory in the eastern European Alps. Austrian Journal of Earth Sciences 105 (2): 78–93.

Kern K., Lieb G.K., Seier G. & Kellerer-Pirklbauer A. 2012. Modelling geomorphological hazards to assess the vulnerability of alpine infrastructure: The example of the Großglockner-Pasterze area, Austria. Austrian Journal of Earth Sciences, 105 (2): 113–127.

Kienast, G., and Kaufmann, V., 2004. Geodetic measurements on glaciers and rock glaciers in the Hohe Tauern National Park (Austria). Proceedings of the 4th ICA Mountain Cartography Workshop, Vall de Núria, Catalonia, Spain, Monografies tècniques 8, Institut Cartogràfic de Catalunya, Barcelona: 77–88.

Kneisel, C. and Hauck, C., 2008. Electrical methods. In: Hauck, C., and Kneisel, C., (eds.): Applied geophysics in periglacial environments. 1–27. Cambridge University Press

Koefoed, O., 1979. Geosounding Principles I, Methods in Geochemistry and Geophysics, 14A, Elsevier, New York.

Krainer, K., Kellerer-Pirklbauer, A., Kaufmann, V., Lieb, G.K., Schrott, L., and Hausmann, H., 2012. Permafrost Research in Austria: History and recent advances. Austrian Journal of Earth Sciences 105 (2): 2–11.

Krysiecki, J.-M., Bodin, X. and Schoeneich, P., 2008. Collapse of the Bérard Rock Glacier (Southern French Alps). In: D.L. Kane and K.M. Hinkel (eds.), Extended Abstracts of the Ninth International Conference on Permafrost (NICOP), University of Alaska, Fairbanks, USA: 153–154.

Lieb, G.K., Kellerer-Pirklbauer, A. and Kleinferchner, H., 2010. Rock glacier inventory of Central and Eastern Austria elaborated within the PermaNET project. Institute of Geography and Regional Science, University of Graz. Digital Media.

Rieckh M. 2011. Monitoring of the alpine snow cover using automatic digital photography – Results from the Hohe Tauern range (Central Austrian Alps). Unpublished Master Thesis, University of Graz, 94 p.

Rieckh M., Kellerer-Pirklbauer A., and Avian, M., 2011. Evaluation of spatial variability of snow cover duration in a small alpine catchment using automatic photography and terrain-based modelling. Geophysical Research Abstracts 13: EGU2011-12048.